




Article

Priming of Colorectal Tumor-Associated Fibroblasts with Zoledronic Acid Conjugated to the Anti-Epidermal Growth Factor Receptor Antibody Cetuximab Elicits Anti-Tumor V δ 2 T Lymphocytes

Jordi Leonardo Castrillo Fernandez ¹, Roberto Benelli ¹, Delfina Costa ¹, Alessio Campioli ^{2,3}, Sara Tavella ^{2,3}, Maria Raffaella Zocchi ^{4,*} and Alessandro Poggi ^{1,*}

¹ Molecular Oncology and Angiogenesis Unit, IRCCS Ospedale Policlinico San Martino, 16132 Genoa, Italy

² Cellular Oncology Unit, IRCCS Ospedale Policlinico San Martino, 16132 Genova, Italy

³ Department of Experimental Medicine, University of Genoa, 16132 Genoa, Italy

⁴ Division of Immunology, Transplants and Infectious Diseases, IRCCS San Raffaele Scientific Institute, 20132 Milan, Italy

* Correspondence: zocchi.maria@hsr.it (M.R.Z.); alessandro.poggi@hsanmartino.it (A.P.); Tel.: +39-010-5558433 (A.P.)

Simple Summary: Different cells present in the tumor microenvironment can deeply influence both cancer spreading and the success of therapy in solid tumors, including colorectal carcinoma (CRC). In particular, tumor-associated fibroblasts (TAF) exert potent immunosuppressive effects leading to the impairment of anti-tumor surveillance and interfering with the function of therapeutic antibodies. Herein, we show that CRC-derived TAF can be turned by zoledronic acid (ZA), in soluble form or as antibody-drug conjugate (ADC), into efficient stimulators of anti-tumor lymphocytes. The ADC, made of the anti-EGFR cetuximab (Cet), used in CRC therapy, and ZA (Cet-ZA) can induce the proliferation of lymphocytes that become able to kill both tumor cells and TAF. The double result is a direct anti-cancer effect and the neutralization of the inhibitory activity exerted by its stroma. The major advantage of the Cet-ZA ADC formulation is the precise delivery of ZA to EGFR⁺ cells, targeting TAF (potentially immunosuppressive), besides CRC cells.

Abstract: Tumor-associated fibroblasts (TAF) exert immunosuppressive effects in colorectal carcinoma (CRC), impairing the recognition of tumor cells by effector lymphocytes, including V δ 2 T cells. Herein, we show that CRC-derived TAF can be turned by zoledronic acid (ZA), in soluble form or as antibody-drug conjugate (ADC), into efficient stimulators of V δ 2 T cells. CRC-TAF, obtained from patients, express the epidermal growth factor receptor (EGFR) and the butyrophilin family members BTN3A1/BTN2A1. These butyrophilins mediate the presentation of the phosphoantigens, accumulated in the cells due to ZA effect, to V δ 2 T cells. CRC-TAF exposed to soluble ZA acquired the ability to trigger the proliferation of V δ 2 T cells, in part represented by effector memory cells lacking CD45RA and CD27. In turn, expanded V δ 2 T cells exerted relevant cytotoxic activity towards CRC cells and CRC-TAF when primed with soluble ZA. Of note, also the ADC made of the anti-EGFR cetuximab (Cet) and ZA (Cet-ZA), that we recently described, induced the proliferation of anti-tumor V δ 2 T lymphocytes and their activation against CRC-TAF. These findings indicate that ZA can educate TAF to stimulate effector memory V δ 2 T cells; the Cet-ZA ADC formulation can lead to the precise delivery of ZA to EGFR⁺ cells, with a double targeting of TAF and tumor cells.

Keywords: tumor associated fibroblasts; antibody-drug conjugate; colorectal cancer; epidermal growth factor receptor; gammadelta T lymphocytes; amino-bis-phosphonates



Citation: Fernandez, J.L.C.; Benelli, R.; Costa, D.; Campioli, A.; Tavella, S.; Zocchi, M.R.; Poggi, A. Priming of Colorectal Tumor-Associated Fibroblasts with Zoledronic Acid Conjugated to the Anti-Epidermal Growth Factor Receptor Antibody Cetuximab Elicits Anti-Tumor V δ 2 T Lymphocytes. *Cancers* **2023**, *15*, 610. <https://doi.org/10.3390/cancers15030610>

Academic Editors: Yasushi Shintani, Toru Kimura and Ryu Kanzaki

Received: 19 December 2022

Revised: 13 January 2023

Accepted: 16 January 2023

Published: 18 January 2023



Copyright: © 2023 by the authors. Licensee MDPI, Basel, Switzerland. This article is an open access article distributed under the terms and conditions of the Creative Commons Attribution (CC BY) license (<https://creativecommons.org/licenses/by/4.0/>).

1. Introduction

It is widely accepted that the tumor microenvironment (TME) can deeply influence the onset and development of cancers. In particular, mesenchymal stromal cells (MSC) are known to exert potent immunosuppressive effects leading to the downregulation of immune cell function and impairing anti-tumor immune responses [1–3]. Indeed, the interaction between MSC isolated from healthy bone marrow and effector lymphocytes can lead to the suppression of T cell proliferation and cytotoxic activity [4–6]. MSC present within the tumor, are mostly tumor-associated fibroblasts (TAF), myofibroblasts, pericytes and adipocytes [6,7]. MSC also populate healthy tissues; in a normal gut they are a structural component of intestinal crypts and regulate epithelial cell proliferation [8,9]. According to these characteristics, MSC are considered main actors of carcinogenesis [10,11]. In colorectal cancer (CRC), TAF are known to actively contribute to imbalance anti-cancer surveillance towards immunosuppression and consequent tumor growth [12–14]. Thus, both MSC and TAF are considered attractive targets for anti-tumor therapies aimed to modify TME and promote immunocompetent cell function [15–17]. As an example, fibroblast activation protein has been proposed as a component of an anti-tumor vaccine resulted as efficient in a murine model, leading to tumor infiltration of CD8⁺ T cells, reduction of TAF number and inhibition of the recruitment of immunosuppressive cells within the tumor [16].

We have reported that CRC-TAF can impair the recognition of CRC by anti-tumor effector cells [18–20]; among them are V δ 2 T lymphocytes, a circulating T cell population recruited to the tumor site in several cancers, including CRC [21–23]. These lymphocytes can be triggered by zoledronic acid (ZA), that is taken up by antigen-presenting cells such as monocytes or cancer cells, and induce accumulation of pyrophosphate antigens (PA) through interference with the mevalonate pathway [24,25]. Subsequently, PA are exposed on the CRC cell surface by the butyrophilin subfamily 3 member A1 and subfamily 2 member A1 (BTN3A1/BTN2A1) and presented to the T cell receptor (TCR) of V δ 2 T cells [26,27]. For this reason, aminobisphosphonates (N-BPs), including ZA, have been proposed as useful tools in cancer immunotherapy [28–30]. We also demonstrated that N-BPs, acting on the mevalonate biosynthetic pathway, can regulate MSC-induced T-cell suppression and B-lymphocyte survival [31].

More importantly, we reported that the exposure of CRC to ZA, soluble or nanoformulated, leads to the expansion of V δ 2 T lymphocytes with effector memory phenotype and sensitizes cancer cells to $\gamma\delta$ T cell-mediated cytotoxicity [19,32,33]. Furthermore, BTN3A1 is detected in CRC at the tumor site, on epithelial and stromal cells, often close to areas infiltrated by V δ 2 T lymphocytes, making conceivable the use of N-BPs in therapeutic schemes against CRC [19]. An important constraint of these drugs is represented by their preferential localization in the bone marrow [28,29]. To enhance N-BPs tumor targeting, besides the nanoformulated ZA [33], we recently proposed a novel antibody-drug conjugate (ADC), made of ZA and the therapeutic anti-epithelial growth factor receptor (EGFR) antibody cetuximab (Cet) [34]. CRC organoids primed with Cet-ZA ADC could trigger the expansion of V δ 2 T cells from peripheral blood and tumor-infiltrating lymphocytes, able to exert autologous tumor cell killing [34].

In this work, we show that CRC-TAF exposed to soluble ZA or Cet-ZA ADC become able to trigger the proliferation of V δ 2 T cells, starting from purified T lymphocytes. The expanded V δ 2 T cell population was in part represented by effector memory cells that exerted relevant cytotoxic activity towards CRC cells and CRC-TAF when primed with ZA or Cet-ZA. These findings indicate that the Cet-ZA ADC formulation can lead to the precise delivery of ZA to EGFR⁺ cells, targeting TAF besides CRC cells and inducing a pro-stimulatory instead of an inhibitory function.

2. Materials and Methods

2.1. TAF Isolation from Tumor Specimens

CRC specimens were obtained from 20 patients (see Table S1) during therapeutic surgery at the Surgical Oncology Unit, IRCCS Ospedale Policlinico San Martino, Genoa,

upon signed informed consent (Institutional and Regional Ethic Committee approval, PR163REG2014, renewed in 2017). This cohort of CRC patients was composed of newly-diagnosed patients without any kind of therapeutic treatment before surgery. Samples were anonymized as reported and referred in the paper with the year and serial number for brevity [33]; all these CRC-TAF have been used within the 8–9th culture passage.

Primary TAF lines were obtained by mincing CRC mucosa, enzyme digestion and debris removal by soft centrifugation as reported [35]; cell suspensions were then purified by density gradient centrifugation (Lympholyte, Cederlane, Burlington, ON, Canada) and seeded in culture wells for 36 h. Non-adherent cells were removed and adherent cells showing a fibroblast-like morphology were cultured for an additional 7 d in MEMalpha (Euroclone, Milan, Italy) supplemented with 10% foetal calf serum (FCS, Sigma Chemicals Co., St. Louis, MO, USA). At confluence, cell cultures were split and expanded as described [19,31]. Phenotype for Intercellular Adhesion Molecule 1 (ICAM1), Fibroblast Activation Protein (FAP), Thy-1 Cell Surface Antigen (CD90), Endoglin (CD105), Epidermal Growth Factor Receptor (EGFR) and Epithelial Cell Adhesion Molecule (EPCAM) markers were analyzed by indirect immunofluorescence at different time points, along a culture period of two months as described in Section 2.5. TAF were also tested for the expression of BTN3A1 and BTN2A1.

2.2. ZA and Cet-ZA ADC

Zoledronic acid (ZA, MW 272.09) was purchased from Selleckchem (Houston, TX, USA), while Cet (Erbix[®]) was obtained as a left-over of the preparation used for CRC patients' therapy (kind gift from the Pharmacy Unit of IRCCS Ospedale Policlinico San Martino, Genoa). Cet-ZA ADC was prepared by Nanovex Biotechnologies (Asturias, Spain) as reported in [34]. Briefly, Erbix[®] was dialyzed to eliminate the excipients, while ZA and 1-ethyl-3-(3-dimethylaminopropyl) carbodiimide hydrochloride (EDC, Sigma Aldrich, St. Louis, MO, USA) were prepared in 0.1 M imidazole at pH 6 ± 0.2 (with HCl 1 N). ZA has been incorporated into Cet structure exploiting the phosphoric groups of ZA according to the reactions reported to conjugate peptides and the free phosphoric acid of DNA. Cet-ZA was then purified from free imidazole, EDC and ZA through dialysis with the Slide-A-Lyzer Cassette (Thermo Fisher Italia, Monza, Italy) at 10,000 MWCO for 24 h. The resulting link between ZA and Cet is covalent in the absence of a linker molecule. The drug antibody ratio was 4.3 as determined by matrix assisted laser desorption ionization mass spectrometry [34].

2.3. CRC-TAF/T Cell Co-Cultures

Peripheral blood mononuclear cells (PBMC) were isolated from venous blood samples of healthy donors of the Transfusional Centre of the IRCCS Ospedale Policlinico San Martino (provided signed institutional informed consent, defined by the Regional Ethic Committee, CONSAZH780148/17 July 2015) by density gradient separation [36]. Monocytes (Mo) and T lymphocytes were purified from PBMC with the specific negative separation kits (Rosettesep, StemCell Technologies, Vancouver, BC, Canada), with a yield of >75% pure for CD14⁺ Mo or >98% of CD2⁺CD3⁺ T cells (Figure S1). The CD2⁺CD3⁺ T cells were incubated overnight in RPMI 1640 (supplemented with 10% FBS, Penicillin/Streptomycin and L-Glutamine, all from Gibco) to discard by adherence any residual Mo component and to avoid their presence in stimulation experiments. Purified T lymphocytes were added to either TAF or Mo, previously seeded overnight into 96 w U-bottomed plates (Sarstedt, Nümbrecht, Germany), at T:TAF ratios as indicated (from 20:1 to 1000:1), or at a T:Mo ratio of 200:1, according to our published data [33], without or with 2.5 µg/mL Cet-ZA or 1.2 µM ZA. Titration experiments using ZA at 2.5 to 0.6 µM were also performed as described in [33]. After 24 h, at 37 °C in a humidified 5% CO₂ incubator, human recombinant interleukin 2 (IL-2, Peprotech-Thermo Fisher, 30 IU/10 ng/mL final concentration, Waltham, MA, USA) was added and co-cultures were continued up to 21 days. The concentration of Cet-ZA for functional experiments was determined on the basis of the EC₅₀ as reported [34].

2.4. V δ 2 T Cell Proliferation

To measure the proliferation of V δ 2 T lymphocytes, purified T cells were labelled with CFSE as described in [31]. Briefly, 10^6 cells were incubated for 30 min at 37 °C in a water bath, in a complete medium with 100 nM CFSE. Then, cells were extensively washed and put in co-cultures as described in Section 2.3, with or without ZA (1.2 μ M or as reported in Section 2.3 for T:TAF and T:Mo co-cultures) or Cet-ZA (2.5 μ g/mL). At 10 or 20 d, the percentage of V δ 2 T lymphocytes was evaluated by flow cytometry after labelling with the anti-V δ 2 specific mAb $\gamma\delta$ 123R3 (IgG1) [33] followed by Alexafluor 647 goat anti-mouse (GAM). Samples were analyzed on a Cytoflex S flow cytometer and the proliferation was indicated by the reduction of CFSE in the cell generations (G) compared to the content of CFSE in the parental (P) component as evaluated by the FlowJoTM software v 10 (Becton Dickinson, Ashland, OH, USA).

2.5. Immunofluorescence and Flow Cytometry

For V δ 2 T lymphocytes identification, the anti-T cell receptor (TCR) V δ 2 $\gamma\delta$ 123R3 (IgG1) and the anti-CD3 JT3A 289/11/F10 (IgG2a) mAb were used, followed by PE-GAM IgG1 or APC-GAM IgG2a (Thermo Fisher Scientific, Waltham, MA, USA). V δ 2 T cells present in cell culture were also characterized by polychromatic immunofluorescence using anti-V δ 2, anti-CD27 (LT27, IgG2a; Bio-Rad, Hercules, CA, USA) and anti-CD45RA (HI100, IgG2b; Bio-Rad) [33] mAb followed by anti-isotype-specific alexafluor 488 or PE or alexafluor 647 conjugated GAM, respectively. Immunofluorescence on CRC TAF was performed with the anti-ICAM1 (14D2D12, IgG1) [31] mAb, anti-CD90 (FAB2067p, IgG2a, R&D Bio-technie, Minneapolis, MN, USA) mAb, the anti-CD105 mAb (from the producing hybridoma purchased from the American Type Culture Collection, ATCC, Manassas, VA, USA), the anti-EPCAM mAb (ab98003, IgG1, Abcam, MA, USA), the anti-FAP mAb (F11-24, IgG1, eBioscience, San Diego, CA, USA), followed by anti-isotype GAM antisera (Southern Biotechnology, CA, USA) conjugated with alexafluor 647 (Invitrogen, Thermo Fisher Scientific). Control samples were stained with fluorophore-conjugated isotype control mAbs or isotype-matched irrelevant mAb (Becton Dickinson, Palo Alto, CA, USA) followed by anti-isotype-specific GAM-alexafluor 647. The expression of butyrophilins was checked using the rabbit anti-BTN2A1 (1:300, Bioss Antibodies, MA, USA) or the rabbit anti-BTN3A1 (1:200, NovusBio. R&D Bio-technie) followed by a fluorescein-conjugated anti-rabbit antiserum (ThermoFisher, Waltham, MA, USA). For cytoplasmic staining of BTN3A1 and BTN2A1, cells were first fixed with 4% paraformaldehyde, washed and permeabilized with 1% Triton-X100. The anti-EGFR Cet or the Cet-ZA ADC were incubated for 1 h at RT, followed by the APC-labelled anti-human Ig (APC- α -hIg) antiserum. Controls aliquots were stained with APC- α -hIg antiserum. Samples were run on Cytoflex S flow cytometer (Beckman-Coulter, Pasadena, CA, USA), analyzed with the CytExpert 2.4 computer program (Beckman Coulter) and results expressed as Log fluorescence intensity vs. number of cells (MFI, arbitrary units, a.u.) or percentage of positive cells [33].

2.6. Confocal Microscopy

For confocal microscopy, CRC-TAF were plated in 96 w clear flat-bottomed black well plates for imaging (Eppendorf, Merck KGaA, Darmstadt, Germany) and incubated with 2.5 μ g/mL/ 10^6 cells Cet-ZA ADC for 1 h at RT, followed by the APC- α -hIg antiserum and 100 nM Syto16 counterstaining (Thermo Fisher Scientific). To show Cet-ZA internalization, samples were incubated with the ADC as above at 37 °C for 48 h, fixed with 1% PFA, permeabilized with 1% Triton X-100, followed by FITC- α -hIg antiserum, anti-LAMP-1 mAb (clone H4A3, Thermo Fisher Scientific), followed by GAM anti-isotype-specific alexafluor647 antiserum and Syto Orange (40 nM, Thermo Fisher). Samples were observed by the FV500 confocal Laser Scanning Microscope System equipped with Argon, He-Ne green and He-Ne red lasers, associated with IX81 motorized microscope (Olympus Europe GmbH, Hamburg, Germany), using a PlanApo 20X NA1.00 objective. Each image was taken in sequence mode, to avoid the cross-activation of fluorochromes, and data were

analyzed with FluoView computer software v5.0 (Olympus, Tokyo, Japan). Results are shown in pseudocolor as red or green fluorescence vs. nuclei in blue [34].

2.7. Cytotoxicity Assay and Interferon γ (IFN γ) Production

Cytolytic activity of V δ 2 T cells against CRC-TAF or CRC cell lines was tested with the crystal-violet assay as described previously [32]. Target cells were: CRC-TAF 15-066, 16-001, 16-004, 16-027, 16-030, 16-035, or the CRC cell lines HT29, DLD1 (EGFR⁺) and SW620 (EGFR^{dull}) obtained from the cell bank of the IRCCS Ospedale Policlinico San Martino (kind gift of Biological Resource Cell Bank unit, Dr. Barbara Parodi) and correctly identified by the STR DNA profile. The E:T ratio chosen was 10:1 since at this ratio V δ 2 T cells exert low spontaneous anti-tumor cytotoxicity allowing the detection of ZA and Cet-ZA-mediated effect [34]. Experiments were then carried out without or with 2.5 μ g/mL Cet-ZA, or 2.5 μ g/mL Cet, or 1.2 μ M ZA. Indeed, V δ 2 T cell populations used in these experiments were selected for the expression of CD16/Fc γ RIIIa on more than 60% of cells as detected by immunofluorescence. To detect cytotoxicity, after 48 h of incubation surviving cells were stained with crystal-violet and colorimetric intensity was evaluated at the wavelength of 594 nm with the fluorimeter VICTORX5 (Perkin Elmer Italia, Milan, Italy). These OD values were compared to the ones obtained in control CRC cells or TAF cultured alone, as a standard of a 100% viability. A representative example of this procedure for the evaluation of TAF viability is shown in Figure S2.

IFN γ was measured in the supernatant of V δ 2 T cells either alone or co-cultured with CRC-TAF without or with 1.25 μ M ZA or 2.5 μ g/mL Cet-ZA, by ELISA with the specific kit (Peprotech-ThermoFisher). Experiments were carried out at the V δ 2 T:TAF ratio of 10:1 (2×10^5 V δ 2 T cells, 2×10^4 TAF) in 24 well-plates for 48 h, as described [31]. The amount of the IFN γ was expressed as pg/mL referred to a standard curve.

2.8. Immunohistochemistry (IHC) and Digital Image Analysis

Sections of 4- μ m-thick CRC samples were cut and stained with the rabbit anti-BTN2A1 (1:300, Bioss Antibodies) and rabbit anti-BTN3A1 (1:200, NovusBio). IHC was carried out using the automated stainer BOND RX (Leica Biosystem Italia Milan, Italy) according to the manufacturer's instruction as previously described in detail [34]. Digital images were captured using the Aperio AT2 scanner (Leica) under 20X or 40X objective magnification, stored in Aperio E-slide manager, and analyzed using the Aperio Scan Scope software v.102.0.7.5 (Leica Biosystems, Aperio Technologies, Nussloch GmbH, Nußloch, Germany) [34]. Genie Classifier AI software v.1 (Leica Biosystem) was used to identify and quantify the percentage area of each compartment (tumor vs. stroma), excluding empty or adipose tissue areas. Tumor areas were defined by contouring as described [34], considering the central part of the tumor only. The software was trained, using a panel of images manually annotated by the operator, to distinguish the regions of interest (ROI). According to the manufacturer, >95% training accuracy was required for each classifier in order to proceed with the image analysis of cohort samples. The percentage of tumor and stroma was normalized against the total tissue area (mm²) in each image. Two pathologists checked that stromal areas were identified correctly [34,37].

2.9. Statistical Analysis

Data are presented as mean \pm SD as indicated. Statistical analysis was performed using two-tailed unpaired Student's *t* test, with Welch correction, using the GraphPad Prism software 5.0. The cut-off value of significance is indicated in each figure legend.

3. Results

3.1. CRC-TAF Can Stimulate the Expansion of V δ 2 T Cells with Effector Phenotype

First, primary TAF obtained from CRC specimens of 20 patients (Table S1) were analyzed for the expression of different molecules, including mesenchymal or epithelial markers, adhesion molecules, growth factors or ligands for regulating receptors. As shown

in Figure S3 (panel A: two representative cases; panel B: 20 cases), CRC-TAF expressed the fibroblast markers FAP, endoglin (CD105) and the adhesion molecule ICAM1, with a low expression of Thy-1 (CD90). All the CRC-TAF reported in this study expressed EGFR on their surface, while the epithelial marker EPCAM was negative (Figure S3, two representative cases in panel A, 20 cases in panel C). Moreover, they were vimentin and transglutaminase II-positive as described previously both for cultured and in situ fibroblasts [19,20]. This phenotype was checked during the culture and remained stable at least for two months (not shown).

To verify the stimulating effect of ZA, purified T lymphocytes from healthy donors were co-cultured with CRC-TAF at different T:TAF ratios in the presence of 2.5 μ M ZA, concentration in the range 1–5 μ M reported as efficient in our previous papers [19,33], followed by the addition of IL-2. The percentage of V δ 2 T lymphocytes, evaluated at day 10 by flow cytometry with the anti-V δ 2 specific mAb $\gamma\delta$ 123R3, raised in the presence of ZA at the T:TAF ratios of 200:1 or 1000:1 (Figure 1A) suggesting that the drug can be effective on CRC-TAF. The effect of ZA was analyzed for comparison, in co-cultures of T lymphocytes and monocytes since the latter cells are known to accumulate PA in response to N-BPs leading to V δ 2 T lymphocyte proliferation [25,33].

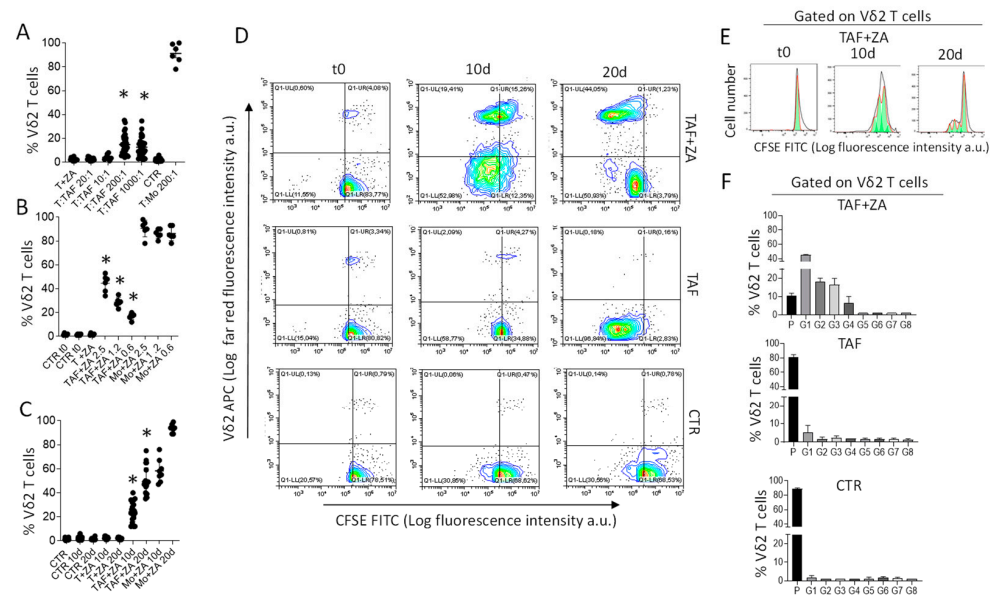


Figure 1. ZA-primed CRC-TAF trigger V δ 2 T cell proliferation. V δ 2 T lymphocytes were identified at day 10 of culture (A) or day 10 and day 20 (B,C) by flow cytometry, and results are expressed as percentage of V δ 2 T cells/total T cells. The mean \pm SD from 20 cases. (A): T lymphocytes from healthy donors ($n = 10$, #19–#28) co-cultured with CRC-TAF ($n = 20$ patients) at the indicated T:TAF ratios without (CTR) or with 2.5 μ M ZA and IL-2. (B): co-cultures of T cells ($n = 2$ #35 and #36) and CRC-TAF ($n = 6$, 016-001, 16-004, 16-030, 16-035, 16-039, 16-047) at T:TAF ratio 200:1 or Mo from healthy donors ($n = 3$, #20, #23, #24) at T:Mo ratio 200:1, without (CTR) or with ZA (from 2.5 μ M to 0.6 μ M). (C): co-cultures of T cells ($n = 10$, #35, #37, #38, #40, #41, #42, #50, #52 #55, #58) and CRC-TAF ($n = 20$, T:TAF ratio 200:1) or Mo (T:Mo ratio 200:1) from healthy donors ($n = 6$), in the absence (CTR) or presence of ZA (1.2 μ M). T + ZA in panels A–C: percentage V δ 2 T cells in cultures of T lymphocytes with 1.25 μ M ZA. (D): V δ 2 T cell proliferation upon a co-culture of T cells from donor #42 labeled with 100 nM CFSE, washed and cultured alone (upper plots) or co-cultured with CRC-TAF 16-030, without (central dot plots) or with 1.2 μ M ZA (lower dot plots). At time 0 (left plots) or at 10 d (central plots) and 20 d (right plots), the percentage of V δ 2 T lymphocytes was evaluated. Percentages of proliferating V δ 2 T cells in the total cell culture are reported in the upper left quadrants of each plot. (E): Cell proliferation analysis of a representative case in the co-culture with T and TAF + ZA experimental condition. (F): percentage of V δ 2 T cells in the parental (P) or subsequent generations (G1–G10) in the culture conditions indicated. In all panels * $p < 0.001$ vs. CTR.

Subsequent titration experiments were performed to define the EC_{50} of ZA in this system evaluated at day 20 to allow further expansion of V δ 2 T cells. T cells were co-cultured with CRC-TAF or with Mo, in the absence or presence of ZA (from 2.5 μ M to 0.6 μ M). V δ 2 T lymphocytes increased in all T:TAF co-cultures, with an EC_{50} of 1.2 μ M in keeping with our previous data [33]. This confirms that CRC-TAF can be exploited as stimulating cells, although with an efficacy lower than that of Mo (Figure 1B). Kinetics experiments showed that the optimal effect of 1.2 μ M ZA was detectable at day 20 (Figure 1C), both for CRC-TAF (range 35–75% V δ 2 T cells) and Mo (>95% V δ 2 T cells). To confirm that V δ 2 T cells detected in the co-cultures were proliferating, another series of experiments was performed using CFSE labeling. Figure 1D depicts an example of these experiments, where CFSE-labelled T cells from donor #42 were cultured alone or co-cultured with CRC-TAF 16-030, without or with 1.2 μ M ZA. At day 20, proliferating V δ 2 T cells identified by the decreased level of CFSE content and reacting with the anti-V δ 2 specific mAb were about 45% (Figure 1D, the upper right plot, upper left quadrant) when co-cultures were primed with ZA compared with <1% without ZA (Figure 1D, central right plot, upper left quadrant). The computerized analysis of gated V δ 2 T cells with decreasing content of CFSE showed that the majority of them was in G1-G3 generation (Figure 1E,F).

We then analyzed the phenotype of the V δ 2 T cell populations obtained after 20 d of culture, focusing on the subsets of naive (N) cells that bear both CD27 and CD45RA molecules, central memory (CM) showing only CD27, effector memory (EM) that are double negative and terminal-differentiated memory cells (TEMRA) that are positive for only CD45RA [19,38,39]. As shown in Figure 2A,B (polychromatic immunofluorescence assay and flow cytometry analysis on V δ 2 gated cells, see Figure S4), the majority of V δ 2 T lymphocytes expanded in co-culture with CRC-TAF exposed to ZA, displayed the phenotype of EM cells (>45% CD45RA⁻ CD27⁻) and of TEMRA (CD45RA⁺CD27⁻). Indeed, at the beginning of the culture, the large majority of V δ 2 T cells were naïve cells and they were converted into TEMRA by the addition of IL2 or IL2 and TAF without ZA (Figure 2B, central graph); whereas EM cells represented a large portion of V δ 2 T cells when triggered with ZA and IL2 (Figure 2B, left).

According to its phenotype, this V δ 2 T cell population could kill the three CRC cell lines tested (HT29, DLD1 and SW620) in the presence of ZA. Moreover, cytotoxic activity was inhibited by the anti-TCR V δ 2 mAb $\gamma\delta$ 123R3 (Figure 2C–E), demonstrating that $\gamma\delta$ TCR is involved in target cell recognition. Furthermore, V δ 2 T lymphocytes activated by co-culture with ZA-treated TAF (V δ 2 T_{AF}), or with Mo exposed to ZA (V δ 2_{Mo}), could kill CRC-TAF at the E:T ratio of 10:1. Moreover, this killing was inhibited by the anti-V δ 2 TCR mAb (Figure 2F,G, respectively) reinforcing the role of TCR in target cell recognition. Altogether, these findings indicate that ZA induces CRC-TAF to stimulate the expansion of anti-tumor effector V δ 2 T lymphocytes that can also exert lytic activity against CRC-TAF.

3.2. Cet-ZA ADC Reacts with CRC-TAF and Induces V δ 2 Cytotoxic Effector T Cells

ZA conjugation with Cet was achieved following the scheme described for the chemical reactions of nucleic acids and proteins, exploiting the synthesis of phosphoramidate; the reactions, leading to a covalent chemical bond between Cet and ZA, have been recently reported [34]. Cet-ZA ADC reactivity was verified by indirect immunofluorescence and flow cytometry using three CRC-TAF (16-001, 16-004 and 16-035) incubated with serial dilutions of the ADC, followed by APC-labelled anti-human Ig antiserum. Figure 3A shows that the reactivity of the ADC (flow cytometry profiles in panel 3B) was comparable to that of native Cet, optimal at 2.5 μ g/mL/10⁶ cells, this concentration was chosen for the functional experiments. Confocal microscopy, depicted in Figure 3C, showed that Cet-ZA ADC was internalized in CRC-TAF and colocalized with the endosomal marker LAMP-1 within 48 h. Figure S5 represents confocal images of Cet-ZA reactivity and cell distribution on three representative CRC-TAF cell lines compared to native Cet.

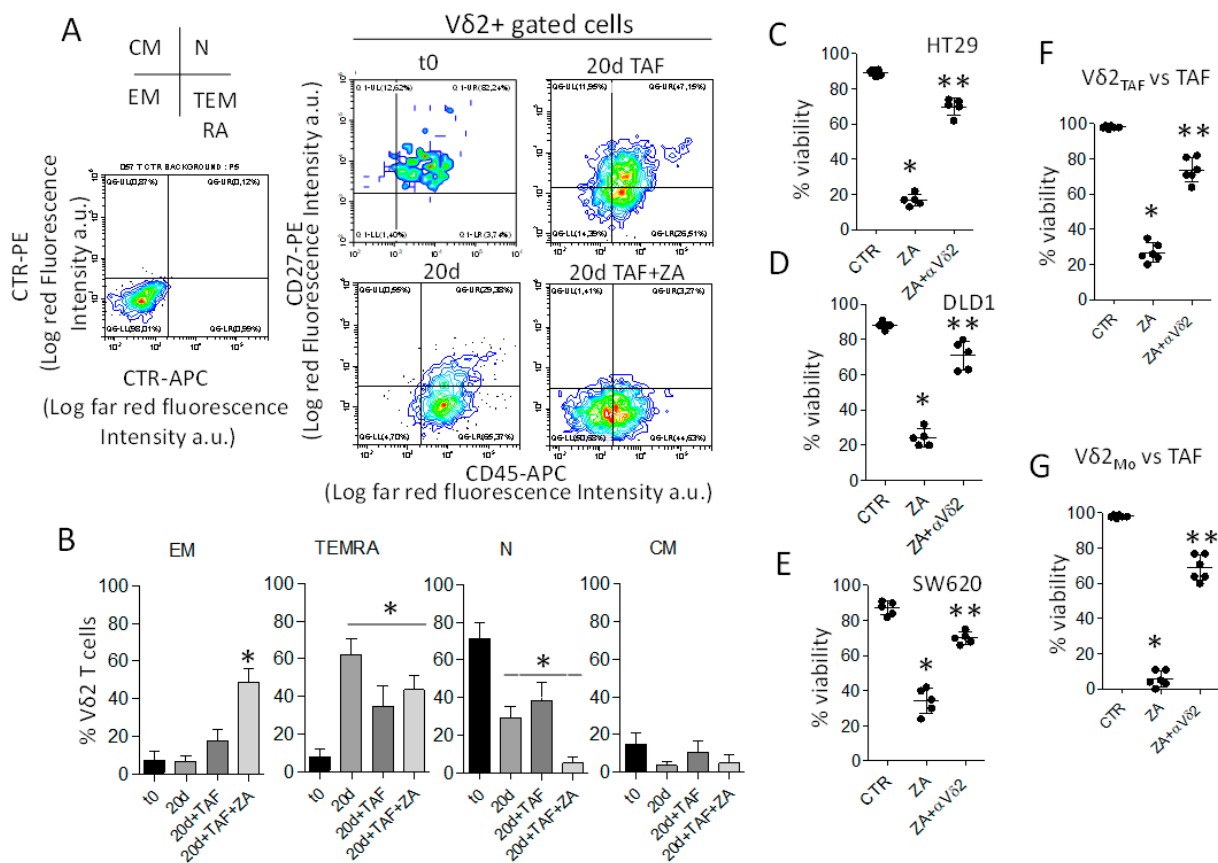


Figure 2. ZA induces CRC-TAF to stimulate the expansion of anti-tumor effector Vδ2 T lymphocytes. (A): Phenotype of Vδ2 T cells (one representative experiment) expanded on untreated or ZA-treated (1.2 μM) CRC-TAF (16-030) on day 20. Samples were labelled with anti-Vδ2, anti-CD27 and anti-CD45RA mAbs gated on Vδ2 T cells and results are expressed as Log far red fluorescence intensity vs. Log red fluorescence intensity. The cross depicted on the left identifies the quadrants showing effector memory (EM, lower left, double negative), terminally-differentiated effector memory (TEMRA, lower right CD45RA⁺ CD27⁻), naive (N, upper right, double positive) and central memory (CM, upper left, CD45RA⁻ and CD27⁺) cells. (B): Analysis of the phenotype of Vδ2 T cells obtained as in A, using T lymphocytes from three healthy donors (#45, #46, #47) co-cultured with six CRC-TAF (016-001, 16-004, 16-030, 16-035, 16-039, 16-047). Results are expressed as percentage of EM, TEMRA, N and CM cells gated on Vδ2 T cells; the mean ± SD from 18 experiments is shown. (C–E): Activated Vδ2 T cells obtained as in A from five healthy donors were tested in a cytotoxicity assay vs. the CRC cell lines HT29 (C) and DLD1 (D) (EGFR⁺) or SW620 (E), EGFR^{du}) at the E:T ratio of 10:1, without (CTR) or with soluble ZA (1.2 μM). In some samples, the anti-Vδ2 TCR mAb was added. Results are expressed as percentage of viability evaluated by crystal-violet assay. (F,G): Activated Vδ2 T lymphocytes from two healthy donors obtained with ZA-activated CRC-TAF (Vδ2 T_{AF}) or monocytes (Vδ2 M₀) were employed as effectors against CRC-TAF (n = 3, 016-001, 16-004, 16-030) as targets at the E:T ratio of 10:1, as above. Cytotoxicity was detected as in panels (C–E), and referred to as percent of viability. * p < 0.001 ZA vs. CTR and ** p < 0.001 ZA + αVδ2 vs. ZA.

We next verified whether Cet-ZA ADC can deliver ZA into CRC-TAF, through the binding with EGFR, and trigger the activation of Vδ2 T cells. To this aim, T lymphocytes purified from healthy donors were co-cultured with CRC-TAF and serial dilution of Cet-ZA (5 μg/mL, 2.5 μg/mL or 1.25 μg/mL) and IL-2. On day 10 of co-culture in the presence of Cet-ZA, an evident increase of the percentage of Vδ2 T cells was detectable. Indeed, the percentage of Vδ2 T cells ranged from 27 to 58 at 5μg/mL of Cet-ZA and the EC₅₀ of the ADC was about 2.5 μg/mL (Figure 4A, 25% Vδ2 T cells vs. <5% without Cet-ZA). Subsequent experiments performed with CRC-TAF and Cet-ZA at 2.5 μg/mL for 10 or

20 days, showed that the latter time point is required to reach the percentage of Vδ2 T lymphocytes ranging between 30 and 58% (Figure 4B, mean 40%), starting from 1–4% of the initial T cell population.

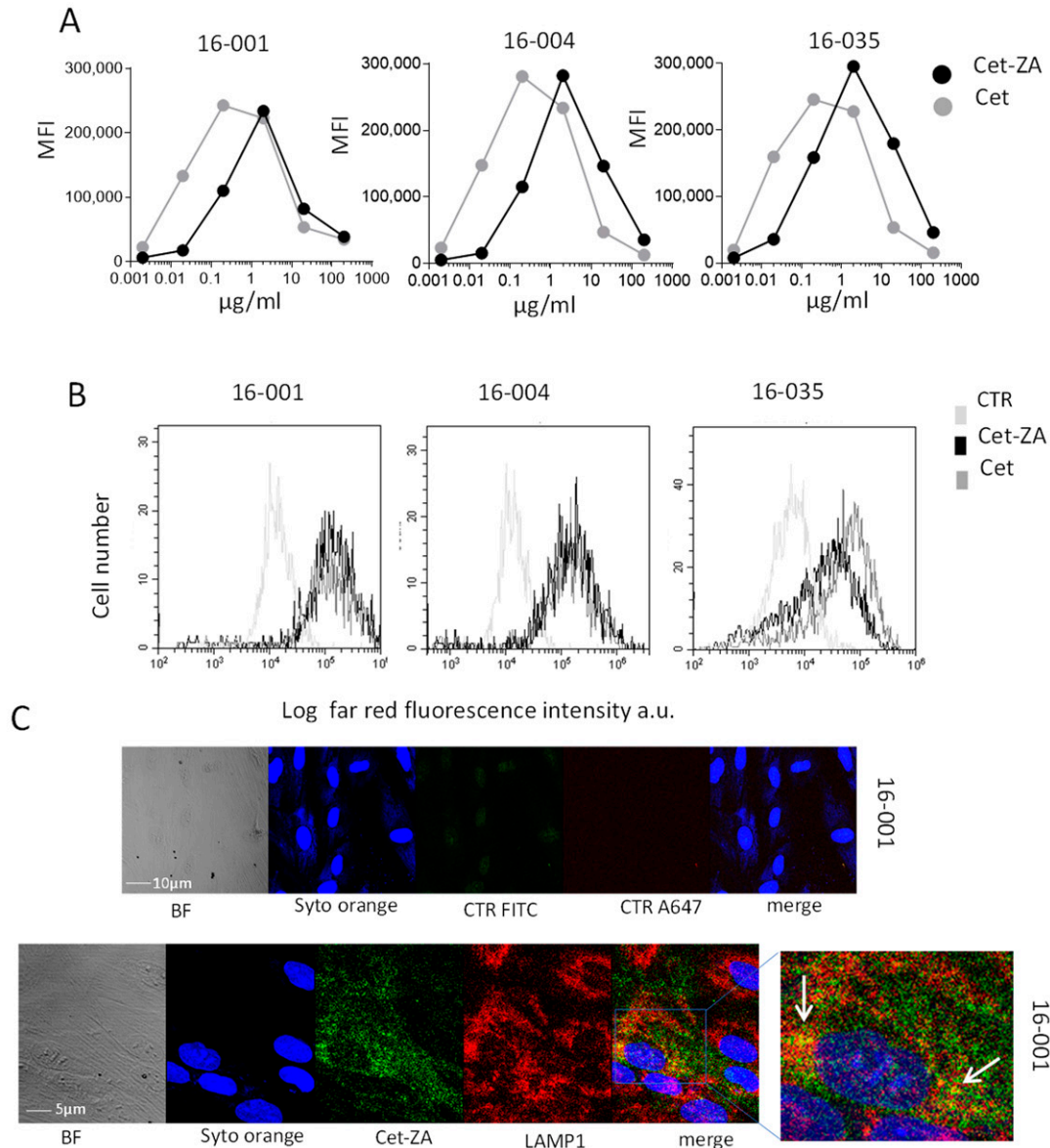


Figure 3. Cet-ZA ADC reactivity with CRC-TAF. **(A):** CRC-TAF (16-001, 16-004 and 16-035), incubated with serial dilutions of Cet-ZA ADC, followed by APC-anti-hIg antiserum were analyzed with the CytExpert 2.4 software and results expressed as mean fluorescence intensity (MFI, a.u.). **(B):** The three CRC-TAF cell lines were incubated with 2.5 µg/mL/10⁶ cells of Cet-ZA ADC (black lines) or native Cet (dark grey lines), followed by APC-anti-hIg antiserum, run on the flow cytometer and analyzed as in A. Results are expressed as Log red fluorescence intensity (MFI, a.u.) vs. number of cells. Cells stained with the second reagent alone (CTR) are shown with light grey lines in each subpanel. **(C):** Upper images show CRC-TAF 16-001 stained with Syto orange alone depicted in blue pseudocolor. Lower images represent Cet-ZA internalization. Blue pseudocolor: nuclei evidenced by Syto Orange; green: Cet-ZA reactivity; red: anti-LAMP-1 mAb reactivity. The enlargement of merge staining is shown on the **right**. White arrows: colocalization of Cet-ZA and LAMP-1 (yellow). BF: bright field. Merge: overlay of blue, green and red fields. Samples were observed by the FV500 confocal Laser Scanning Microscope System using a PlanApo 20X NA1.00 objective. Images were taken in sequence mode to avoid cross-talk between the fluorochromes.

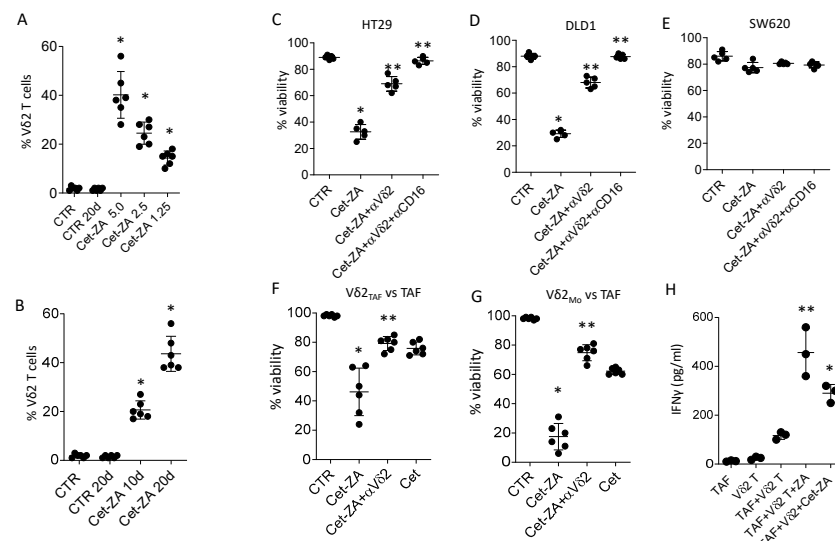


Figure 4. Cet-ZA can expand anti-tumor Vδ2 T cells and stimulate cytolytic activity. (A): Purified T lymphocytes from healthy donors (#49, #50) were co-cultured with CRC-TAF 16-001, or 16-004 or 16-035 without (CTR) or with Cet-ZA (5 µg/mL, 2.5 µg/mL or 1.25 µg/mL) and IL-2 and analyzed on day 10 by flow cytometry. Results are expressed as percentage Vδ2 T lymphocytes; the mean ± SD from 6 experiments is also shown. (B): Experiments performed as in A without (CTR) or with Cet-ZA at 2.5 µg/mL for 10 or 20 days; results expressed as percentage of Vδ2 T lymphocytes also showing the mean ± SD from 6 experiments from co-cultures of T (#51, #52 and CRC-TAF (16-001 or 16-004 or 16-035)). (C–E): Activated Vδ2 T cells obtained from healthy donors ($n = 5$) were used as effectors in cytotoxicity assay vs. HT29 or DLD1 ((C,D), EGFR⁺) or SW620 (E, EGFR^{dull}) without (CTR) or with Cet-ZA (2.5 µg/mL) or Cet (2.5 µg/mL) or soluble ZA (1.2 µM). In some samples the anti-Vδ2 TCR mAb or the anti-CD16 mAb were added (1 µg/mL). Cytotoxicity was detected by crystal-violet staining and expressed as percent of viability. (F,G): Activated Vδ2 T lymphocytes obtained with ZA-activated CRC-TAF (Vδ2 T_{AF}) or monocytes (Vδ2_{Mo}) were employed as effectors against CRC-TAF as above. Cytotoxicity was detected and expressed as in (C–E). (H): IFNγ measured in the supernatant of Vδ2 T cells (#50) either alone or co-cultured with CRC-TAF (16-001 or 16-030 or 16-035), without or with 1.25 µM ZA or 2.5 µg/mL Cet-ZA, by ELISA. Results are expressed as pg/mL referred to a standard curve. In (A–G) panels: * $p < 0.001$ vs. CTR, ** $p < 0.001$ vs. Cet-ZA. In (H) panel: ** $p < 0.004$ vs. TAF + Vδ2 T and * $p < 0.001$ vs. TAF + Vδ2 T.

To analyze the ability of Cet-ZA to elicit Vδ2 T cell-mediated anti-tumor activity, the Vδ2 T cell populations obtained from healthy donors as described in Section 3.1 were used as effectors in cytotoxicity assay. Five populations enriched at 60% of Vδ2 T lymphocytes were chosen and challenged with the CRC cell lines HT29 and DLD1 (EGFR⁺), or SW620 (EGFR^{dull}). Figure 4 shows that in the presence of Cet-ZA the percentage of viable HT29 and DLD1 cells (Figure 4C,D) significantly decreased to 30% in co-cultures with Vδ2 T lymphocytes. This effect was stronger than that obtained with native Cet (40–50% of viable CRC cells, not shown). The EGFR^{dull} SW620 cell line was less sensitive to the effect of Cet-ZA (Figure 4E), nevertheless it was still responsive to soluble ZA (Figure 2C). Of note, the anti-Vδ2 TCR mAb and the combination of anti-Vδ2 plus anti-CD16 mAbs could significantly inhibit Cet-ZA-induced cytotoxicity (Figure 4C,D) indicating that the ADC can activate tumor cell killing by both TCR and FcγRIIIA. In another series of experiments, Vδ2 T lymphocytes activated with ZA-treated TAF (Vδ2 T_{AF}) were employed as effectors against CRC-TAF as above. As shown in Figure 4F, Cet-ZA elicited a significant anti-TAF killing (viability decreased to 20–60%) that was higher than that elicited by native Cet (80% TAF viability) and was inhibited by the anti-Vδ2 TCR mAb, as occurred for soluble ZA (see Figure 2). Activated Vδ2 T cells obtained on ZA-activated monocytes (Vδ2_{Mo}) are shown in Figure 4G for comparison. Furthermore, in this case, Cet-ZA was more effective than native Cet in triggering anti-TAF lytic activity (viability decreased to 5–30% vs. 60% of

native Cet) that was significantly reduced by the anti-V δ 2 mAb. Interestingly, both ZA and Cet-ZA elicited the release of an antitumor cytokine such as IFN γ [39] in the supernatant of V δ 2:TAF co-cultures (Figure 4H); this finding supports that Cet-ZA ADC can stimulate and amplify the antitumor response mediated by V δ 2 T lymphocytes.

3.3. CRC-TAF Express In Situ BTN3A Molecules in Stromal Areas within the Tumor

To support the idea that targeting TAF with ZA or Cet-ZA can be exploited for anti-CRC treatment, the stromal areas of CRC specimens were analyzed by IHC for butyrophilin expression. BTN3A1 or BTN2A1 expression was examined by digital pathology, as reported [34]. BTN2A1 was significantly expressed on cells with fibroblast morphology (Figure 5A,B 17-050 representative case), while BTN3A1 was barely detectable by IHC (Figure 5C, 15-073 representative case). The percentage area of each compartment (tumor vs. stroma) was determined in the CRC specimens with the pattern recognition tool of the Genie Classifier software v.1. Data refer to the areas defined in each slide by contouring the central part of the tumor (CT) as previously described [34]. Results in Figure 5D indicate that stromal areas are significantly higher than tumor zones, thus highlighting the relevance of TME. Of note, the cultured CRC-TAF cell lines 16-004, 16-016, 16-035 expressed BTN2A1 on their surface and in the cytoplasm, evidenced by immunofluorescence and flow cytometry (Figure 5E,F), whereas BTN3A1 membrane and cytoplasmic expression was less detectable (Figure 5E,F). These data point to the potential importance of butyrophilin expression in CRC stromal areas that represent a relevant fraction of the whole tumor tissue.

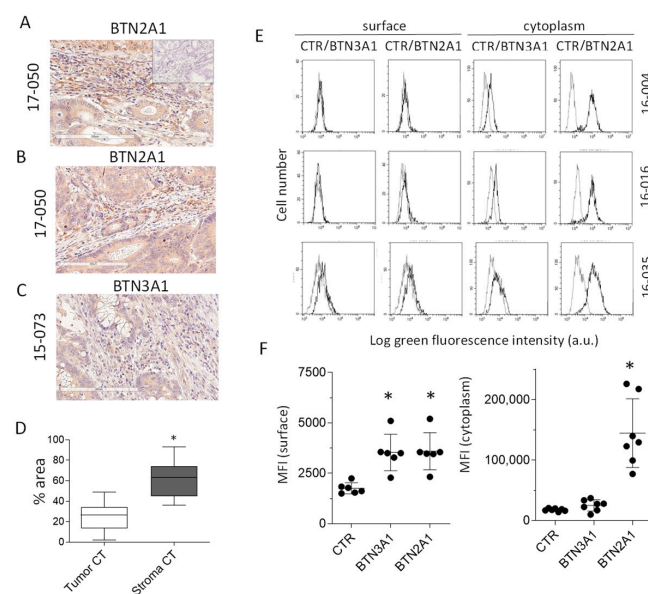


Figure 5. Expression of butyrophilins on tumor stroma and cultured CRC-TAF. (A–C): Sections of the CRC 17-050 or 15-073 were stained with the rabbit anti-BTN2A1 (two fields of 17-050 in (A,B)) or the rabbit anti-BTN3A1 (15-073, (C)) antisera respectively. Digital images (20 \times) were captured using the Aperio AT2 scanner. Negative control in the inset of A. (D): Samples acquired as in (A–C) were analyzed with the pattern recognition tool of the Genie Classifier software and the percentage area of each compartment (tumor vs. stroma) was calculated specifically in the central tumor. The results are the mean \pm SD from 6 different CRC specimens, each analyzed in 4 slide areas. * $p < 0.001$. (E) **Left:** CRC-TAF (16-004,16-016,16-035) were surface stained with the anti-BTN2A1 or the anti-BTN3A1 antisera, followed by FITC-anti-rabbit antiserum. (E) **Right:** the same samples were fixed and permeabilized before staining. Samples were analyzed by flow cytometry and results expressed as the Log green fluorescence intensity vs. number of cells (MFI, arbitrary units, a.u.). Grey histograms: negative control (CTR); black histograms: BTN2A1 or BTN3A1. (F): MFI of BTN3A1 and BTN2A1 in six CRC-TAF stained at the surface (**left**) or in the cytoplasm (**right**). Mean \pm SD of the six cases; * $p < 0.001$.

4. Discussion

Two important problems of cancer immunotherapy are the overcoming of a suppressive TME and the specific targeting of tumor cells. In this paper, we show that we can use a new ADC, made of the N-BP ZA and the anti-EGFR cetuximab [34], to bypass both these limits. Here, we demonstrate that Cet-ZA ADC can react with CRC-TAF expressing EGFR, making them able to stimulate V δ 2 T lymphocytes with effector phenotype and anti-tumor function. On the other side, these effectors are able to kill also CRC-TAF, thus limiting the potential suppressive activity of TME.

We recently published the synthesis, the reactivity and the function of this Cet-ZA ADC in a 3D model of human CRC organoids, showing that it is internalized and localized in the endocytic compartment in tumor cells, as occurs in general for ADC whose processing follows the route of the antibody [34,40]. The advantage of this type of ADC, based on a pH-cleavable phosphoramidate linker for the conjugation, is the delivery of the payload inside the cell, where it can exert its function [41]. This is relevant for ZA, as it acts on the mevalonate pathway inducing the production of the PA isopentenyl pyrophosphate by cells, either antigen-presenting or tumor cells, that in turn stimulate V δ 2 T lymphocytes [24,25]. Accordingly, Cet-ZA is internalized in CRC-TAF colocalizing with the endocytic marker LAMP-1, although the kinetics of internalization in TAF is slower (24–48 h) than in CRC cells (1–2 h) [34].

CRC-TAF are equipped to allow ZA, either soluble or driven by the ADC, to exert its effect: they express BTN2A1, and to a lesser extent BTN3A1 molecules that are needed for the exposure of PA in a molecular form recognizable by the V δ 2 TCR [26,27]. Thus, CRC-TAF exposed either to soluble ZA or to Cet-ZA ADC, can elicit the proliferation of V δ 2 T lymphocytes displaying the phenotype of effector-memory cells, that is cells mostly CD45RA⁺ CD27⁺. Interestingly, PA accumulation occurring in antigen presenting cells and in cancer cells following N-BPs exposure, has been reported to drive not only proliferation, but also maturation of V δ 2 T lymphocytes from naïve to memory cells [39,42]. These lymphocytes are able to kill both tumor cells and CRC-TAF themselves, thus resulting in a regulatory feedback, besides a direct anti-cancer function.

In particular, the cytotoxicity triggered by Cet-ZA ADC is both TCR-mediated, due to the PA production consequent to ZA effect, and antibody-mediated (ADCC), due to Cet binding to Fc γ RIIIA/CD16. The latter type of killing is typical of several different immune effectors, including natural killer cells and macrophages [20,43], and represents a mechanism widely exploited for the pharmacological function of therapeutic antibodies [43,44]. Moreover, the double action of this ADC provides a dual gun to kill tumor cells, on one side, and down-regulate the function of CRC-TAF on the other side. We have already reported that N-BPs, acting on lymph-node mesenchymal stromal cells, can induce V δ 2 T helper1/effector memory lymphocytes and rescue the recognition and killing of lymphoma cells, facilitating rituximab-induced ADCC [39]. Cet-ZA ADC brings together the ability to stimulate effector/memory cells, elicit antitumor activity and allow the action of the therapeutic mAb. At the tumor site, where TAF, V δ 2 T lymphocytes and cancer cells are close one to each other, Cet-ZA can turn TAF into stimulators of effectors that first eliminate stromal cells that may interfere with anti-cancer immune response, and then become effective cancer killers.

ZA/Cet-ZA effect on V δ 2 T cell proliferation is not evident at the lowest T:TAF ratios conceivably due to the reported inhibiting action exerted by fibroblasts or mesenchymal stromal cells on leukocyte function [4]. Nevertheless, Cet-ZA-elicited cytotoxicity is detectable also at low E:T ratio according to what observed for soluble ZA in the present work and previous reports [39]. We can hypothesize that effector lymphocytes proliferated in areas poor of stromal cells can exert antitumor activity also in areas enriched with TAF.

We have recently described ZA-encapsulated nanoparticles (ZA-SPN) as a drug formulation suitable to direct ZA preferentially into the tumor site avoiding the bone tropism of N-BPs [33]. A major advantage of the Cet-ZA ADC towards other drug formulations, including ZA-SPN, is the ability to select, activate and drive an anti-tumor effector cell pop-

ulation into the tumor, due to the specificity of the anti-EGFR Cet, not only avoiding other localizations of ZA, but also targeting only EGFR⁺ cells, either CRC cells or CRC-TAF. A possible drawback is represented by the relative unresponsiveness of CRC cells expressing low levels of EGFR that might allow their escape from the targeting with Cet-ZA. Nevertheless, ZA is delivered precisely inside the cell that has to become the target of immune effectors; afterward, the function of the drug will be enabled provided the expression of the butyrophilins needed to express the PA at the cell surface.

It is of note, that not only cultured CRC-TAF, but also in CRC tissue histology, stromal cells express BTN2A1. BTN3A1 is barely detectable in situ and mainly in the cytoplasm of cultured CRC-TAF, possibly needing an undefined signal (e.g., an inflammatory cytokine) to be expressed by tumor stroma. On the other hand, we reported that BTN3A1 is the main butyrophilin expressed by tumor epithelial cells in CRC [34]. Thus, fibroblasts and tumor cells apparently bear on their membrane different molecules that may cooperate to allow the complete pharmacological action of ZA. This is of interest in the perspective of novel anticancer therapies [45], considering that stroma frequently represents a sizable fraction of tumor tissue and fibroblasts are its principal population. From this viewpoint, a recent report evidenced that TAF produce EGF upon Cet treatment, supporting CRC cell growth and rescuing tumor cells from immunotherapy [46]; thus, CRC-TAF should be considered as targets of therapy to overcome this TME-mediated drug resistance.

5. Conclusions

In conclusion, double targeting of CRC and CRC-TAF by Cet-ZA ADC may represent an interesting therapeutic tool to enhance anti-tumor immunity, restrict the response to the tumor site and convert potential suppressive cells into cooperative anti-cancer agents.

6. Patents

The Cet-ZA ADC is under the Italian patent n. 102022000003758 on 1 March 2022.

Supplementary Materials: The following supporting information can be downloaded at: <https://www.mdpi.com/article/10.3390/cancers15030610/s1>, Figure S1: Supplementary Figure S1. Degree of purity of T lymphocytes and monocytes isolated from PBMC, Figure S2: Evaluation of cytolytic activity of V δ 2 T cells with crystal violet assay; Figure S3: Phenotype of CRC-TAF; Figure S4: Gating strategy to analyze CD45RA and CD27 on V δ 2 T cells; Figure S5: Confocal microscopy of Cet-ZA ADC reactivity with CRC-TAF. Table S1: Pathology features of CRC specimens used in this study to generate TAF primary cell lines.

Author Contributions: Conceptualization, M.R.Z. and A.P.; methodology, J.L.C.F., D.C., A.P., S.T., A.C. and R.B.; software application, R.B. and D.C.; formal analysis, A.P.; investigation, J.L.C.F., A.P., S.T. and A.C.; data curation, A.P. and M.R.Z.; writing—original draft preparation, M.R.Z.; writing—review and editing, R.B., M.R.Z. and A.P.; visualization, A.P.; supervision, A.P. and M.R.Z.; project administration, A.P.; funding acquisition, A.P. All authors have read and agreed to the published version of the manuscript.

Funding: This research was funded by AIRC (Associazione Italiana per la Ricerca sul Cancro) grant number 21648 to AP and by Compagnia di San Paolo (ROL 32567), 5xmille 2015 and 2016 and Ricerca Corrente from the Italian Ministry of Health to AP.

Institutional Review Board Statement: Ligurian Regional Ethic Committee approval, PR163REG2014, renewed in 2017.

Informed Consent Statement: All the human specimens have been obtained after signed informed consent approved by the Ligurian Regional Ethic Committee approval, PR163REG2014, renewed in 2017.

Data Availability Statement: The data and reagents will be available under appropriate and motivated requests upon a material transfer agreement between the IRCCS Ospedale Policlinico San Martino and the other party.

Acknowledgments: The authors thank the Pathology and Pharmacy unit of IRCCS Ospedale Policlinico San Martino for providing tumor specimens and the left-over of the Erbitux (Cetuximab) antibody for the described experiments in this study.

Conflicts of Interest: The authors declare no conflict of interest. The funders had no role in the design of the study; in the collection, analyses, or interpretation of data; in the writing of the manuscript; or in the decision to publish the results.

References

1. Lazennec, G.; Jorgensen, C. Concise review: Adult multipotent stromal cells and cancer: Risk or benefit? *Stem Cells* **2008**, *26*, 1387–1394. [[CrossRef](#)]
2. Krampera, M. mesenchymal stromal cell “licensing”: A multistep process. *Leukemia* **2011**, *25*, 1408–1414. [[CrossRef](#)]
3. Quante, M.; Tu, S.P.; Tomita, H.; Gonda, T.; Wang, S.S.; Takashi, S.; Baik, G.H.; Shibata, W.; Diprete, B.; Betz, K.S.; et al. Bone marrow-derived myofibroblasts contribute to the mesenchymal stem cell niche and promote tumour growth. *Cancer Cell* **2011**, *19*, 257–272. [[CrossRef](#)] [[PubMed](#)]
4. Aggarwal, S.; Pittenger, M.F. Human mesenchymal stem cells modulate allogeneic immune cell responses. *Blood* **2005**, *105*, 1815–1822. [[CrossRef](#)] [[PubMed](#)]
5. Beyth, S.; Borovsky, Z.; Mevorach, D.; Liebergall, M.; Gazit, Z.; Aslan, H.; Galun, E.; Rachmiewtz, J. Human mesenchymal stem cells alter antigen-presenting cell maturation and induce T cell unresponsiveness. *Blood* **2005**, *105*, 2214–2219. [[CrossRef](#)]
6. Poggi, A.; Musso, A.; Dapino, I.; Zocchi, M.R. Mechanisms of tumour escape from immune system: Role of mesenchymal stromal cells. *Immunol. Lett.* **2014**, *159*, 55–72. [[CrossRef](#)] [[PubMed](#)]
7. Turley, S.J.; Cremasco, V.; Astarita, J.L. Immunological hallmarks of stromal cells in the tumour microenvironment. *Nat. Rev. Immunol.* **2015**, *15*, 669–682. [[CrossRef](#)] [[PubMed](#)]
8. Nakayama, H.; Miyazaki, E.; Enzan, H. Differential expression of high molecular weight caldesmon in colorectal pericryptal fibroblasts and tumour stroma. *J. Clin. Pathol.* **1999**, *52*, 785–786. [[CrossRef](#)]
9. Cirri, P.; Chiarugi, P. Cancer-associated-fibroblasts and tumour cells: A diabolic liaison driving cancer progression. *Cancer Metastasis Rev.* **2012**, *31*, 195–208. [[CrossRef](#)]
10. Raffaghello, L.; Dazzi, F. Classification and biology of tumour associated stromal cells. *Immunol. Lett.* **2015**, *168*, 175–182. [[CrossRef](#)]
11. Kalluri, R. The biology and function of fibroblasts in cancer. *Nat. Rev. Cancer* **2016**, *16*, 582–598. [[CrossRef](#)] [[PubMed](#)]
12. Barnas, J.L.; Simpson-Abelson, M.R.; Brooks, S.P.; Kelleher, R.J.; Bankert, R.B. Reciprocal functional modulation of the activation of T lymphocytes and fibroblasts derived from human solid tumours. *J. Immunol.* **2010**, *185*, 2681–2692. [[CrossRef](#)] [[PubMed](#)]
13. Hogan, N.M.; Dwyer, R.M.; Joyce, M.R.; Kerin, M.J. Mesenchymal stem cells in the colorectal tumour microenvironment: Recent progress and implications. *Int. J. Cancer* **2012**, *131*, 1–7. [[CrossRef](#)] [[PubMed](#)]
14. O’Malley, G.; Heijltjes, M.; Houston, A.M.; Rani, S.; Ritter, T.; Egan, L.J.; Ryan, A.E. Mesenchymal stromal cells (MSCs) and colorectal cancer—A troublesome twosome for the anti-tumour immune response? *Oncotarget* **2016**, *7*, 60752–60774. [[CrossRef](#)]
15. Loeffler, M.; Kruger, J.A.; Niethammer, A.G.; Reisfeld, R.A. Targeting tumour associated fibroblasts improves cancer chemotherapy by increasing intratumoural drug uptake. *J. Clin. Investig.* **2006**, *116*, 1955–1962. [[CrossRef](#)]
16. Li, X.; Wang, Y.; Zhao, Y.; Yang, H.; Tong, A.; Zhao, C.; Shi, H.; Li, Y.; Wang, Z.; Wei, Y. Immunotherapy of tumour with vaccine based on basic fibroblast growth factor-activated fibroblasts. *J. Cancer Res. Clin. Oncol.* **2014**, *140*, 271–280. [[CrossRef](#)]
17. Liu, R.; Li, H.; Liu, L.; Yu, J.; Ren, X. Fibroblast activation protein: A potential therapeutic target in cancer. *Cancer Biol. Ther.* **2012**, *13*, 123–129. [[CrossRef](#)]
18. Poggi, A.; Varesano, S.; Zocchi, M.R. How to hit mesenchymal stromal cells and make the tumour microenvironment immunostimulant rather than immunosuppressive. *Front. Immunol.* **2018**, *9*, 262. [[CrossRef](#)]
19. Zocchi, M.R.; Costa, D.; Venè, R.; Tosetti, F.; Ferrari, N.; Minghelli, S.; Benelli, R.; Scabini, S.; Romairone, E.; Catellani, S.; et al. Zoledronate can induce colorectal cancer microenvironment expressing BTN3A1 to stimulate effector $\gamma\delta$ T cells with anti-tumour activity. *Oncoimmunology* **2017**, *6*, e1278099. [[CrossRef](#)]
20. Costa, D.; Venè, R.; Benelli, R.; Romairone, E.; Scabini, S.; Catellani, S.; Rebesco, B.; Mastracci, L.; Grillo, F.; Minghelli, S.; et al. Targeting the Epidermal Growth Factor Receptor Can Counteract the Inhibition of Natural Killer Cell Function Exerted by Colorectal Tumour-Associated Fibroblasts. *Front. Immunol.* **2018**, *9*, 1150. [[CrossRef](#)]
21. Corvaisier, M.; Moreau-Aubry, A.; Diez, E.; Bennouna, J.; Mosnier, J.F.; Scotet, E.; Bonneville, M.; Jotereau, F. V. gamma 9V delta 2 T cell response to colon carcinoma cells. *J. Immunol.* **2005**, *175*, 5481–5488. [[CrossRef](#)]
22. Bonneville, M.; O’Brien, R.L.; Born, W.K. Gammadelta T cell effector functions: A blend of innate programming and acquired plasticity. *Nat. Rev. Immunol.* **2010**, *10*, 467–478. [[CrossRef](#)] [[PubMed](#)]
23. Meraviglia, S.; Lo Presti, E.; Tosolini, M.; La Mendola, C.; Orlando, V.; Todaro, M.; Catalano, V.; Stassi, G.; Cicero, G.; Vieni, S.; et al. Distinctive features of tumour-infiltrating $\gamma\delta$ T lymphocytes in human colorectal cancer. *Oncoimmunology* **2017**, *6*, e1347742. [[CrossRef](#)] [[PubMed](#)]
24. Gober, H.J.; Kistowska, M.; Angman, L.; Jenö, P.; Mori, L.; De Libero, G. Human T cell receptor gammadelta cells recognize endogenous mevalonate metabolites in tumour cells. *J. Exp. Med.* **2003**, *197*, 163–168. [[CrossRef](#)] [[PubMed](#)]

25. Das, H.; Wang, L.; Kamath, A.; Bukowski, J.F. Vgamma2Vdelta2 T-cell receptor-mediated recognition of aminobisphosphonates. *Blood* **2001**, *98*, 1616–1618. [[CrossRef](#)] [[PubMed](#)]
26. Vavassori, S.; Kumar, A.; Wan, G.; Ramanjaneyulu, G.S.; Cavallari, M.; El Daker, S.; Beddoe, T.; Theodossis, A.; Williams, N.K.; Gostick, E.; et al. Butyrophilin 3A1 binds phosphorylated antigens and stimulates human $\gamma\delta$ T cells. *Nat. Immunol.* **2013**, *14*, 908–916. [[CrossRef](#)] [[PubMed](#)]
27. Cano, C.E.; Pasero, C.; De Gassart, A.; Kerneur, C.; Gabriac, M.; Fullana, M.; Granarolo, E.; Hoet, R.; Scotet, E.; Rafia, C.; et al. BTN2A1, an immune checkpoint targeting V γ 9V δ 2 T cell cytotoxicity against malignant cells. *Cell Rep.* **2021**, *36*, 109359. [[CrossRef](#)]
28. Santini, D.; Vespasiani Gentilucci, U.; Vincenzi, B.; Picardi, A.; Vasaturo, F.; La Cesa, A.; Onori, N.; Scarpa, S.; Tonini, G. The antineoplastic role of bisphosphonates: From basic research to clinical evidence. *AnnOncol* **2003**, *14*, 1468–1476. [[CrossRef](#)]
29. Clézardin, P.; Fournier, P.; Boissier, S.; Peyruchaud, O. In vitro and in vivo anti-tumour effects of bisphosphonates. *Curr. Med. Chem.* **2003**, *10*, 173–180. [[CrossRef](#)]
30. Santolaria, T.; Robard, M.; Léger, A.; Catros, V.; Bonneville, M.; Scotet, E. Repeated systemic administration of aminobisphosphonates and human V γ 9V δ 2 T cells efficiently control tumour development in vivo. *J. Immunol.* **2013**, *191*, 1993–2000. [[CrossRef](#)]
31. Musso, A.; Zocchi, M.R.; Poggi, A. Relevance of the mevalonate biosynthetic pathway in the regulation of bone marrow mesenchymal stromal cell-mediated effects on T-cell proliferation and B-cell survival. *Haematologica* **2011**, *96*, 16–23. [[CrossRef](#)] [[PubMed](#)]
32. Varesano, S.; Zocchi, M.R.; Poggi, A. Zoledronate triggers V δ 2 T cells to destroy and kill spheroids of colon carcinoma: Quantitative image analysis of three-dimensional cultures. *Front. Immunol.* **2018**, *9*, 998. [[CrossRef](#)] [[PubMed](#)]
33. Di Mascolo, D.; Varesano, S.; Benelli, R.; Mollica, H.; Salis, A.; Zocchi, M.R.; Decuzzi, P.; Poggi, A. Nanoformulated Zoledronic Acid Boosts the V δ 2 T Cell Immunotherapeutic Potential in Colorectal Cancer. *Cancers* **2019**, *12*, 104. [[CrossRef](#)] [[PubMed](#)]
34. Benelli, R.; Costa, D.; Salvini, L.; Tardito, S.; Tosetti, F.; Villa, F.; Zocchi, M.R.; Poggi, A. Targeting of colorectal cancer organoids with zoledronic acid conjugated to the anti-EGFR antibody cetuximab. *J. Immunother. Cancer* **2022**, *in press*. [[CrossRef](#)]
35. Benelli, R.; Venè, R.; Minghelli, S.; Carlone, S.; Gatteschi, B.; Ferrari, N. Celecoxib induces proliferation and Amphiregulin production in colon subepithelial myofibroblasts, activating erk1-2 signaling in synergy with EGFR. *Cancer Lett.* **2013**, *328*, 73–82. [[CrossRef](#)] [[PubMed](#)]
36. Prevosto, C.; Zancolli, M.; Canevali, P.; Zocchi, M.R.; Poggi, A. Generation of CD4+ or CD8+ regulatory T cells upon mesenchymal stem cell-lymphocyte interaction. *Haematologica* **2007**, *92*, 881–888. [[CrossRef](#)] [[PubMed](#)]
37. Alfano, M.; Locatelli, I.; D'Arrigo, C.; Mora, M.; Voizzi, G.; De Acutis, A.; Pece, R.; Tavella, S.; Costa, D.; Poggi, A.; et al. Lysyl-Oxidase Dependent Extracellular Matrix Stiffness in Hodgkin Lymphomas: Mechanical and Topographical Evidence. *Cancers* **2022**, *14*, 259. [[CrossRef](#)]
38. Dieli, F.; Poccia, F.; Lipp, M.; Sireci, G.; Caccamo, N.; Di Sano, C.; Salerno, A. Differentiation of effector/memory Vdelta2 T cells and migratory routes in lymph nodes or inflammatory sites. *J. Exp. Med.* **2003**, *198*, 391–397. [[CrossRef](#)]
39. Musso, A.; Catellani, S.; Canevali, P.; Tavella, S.; Venè, R.; Boero, S.; Pierri, I.; Gobbi, M.; Kunkl, A.; Ravetti, J.L.; et al. Aminobisphosphonate prevent the inhibitory effect exerted by lymph node stromal cells on antitumour V δ 2 T lymphocytes in non-Hodgkin lymphomas. *Haematologica* **2014**, *99*, 131–139. [[CrossRef](#)]
40. Dean, A.Q.; Luo, S.; Twomey, J.D.; Zhang, B. Targeting cancer with antibody-drug conjugates: Promises and challenges. *mAbs* **2021**, *13*, 1951427. [[CrossRef](#)]
41. Olatunji, F.P.; Herman, J.W.; Kesic, B.N.; Olabode, D.; Berkman, C.E. A click-ready pH-triggered phosphoramidate-based linker for controlled-release of monomethyl auristatin E. *Tetrahedron. Lett.* **2020**, *61*, 152398. [[CrossRef](#)]
42. Angelini, D.F.; Borsellino, G.; Poupot, M.; Diamantini, A.; Poupot, R.; Bernardi, G.; Poccia, F.; Fournié, J.J.; Battistini, L. Fc γ RIII discriminates between 2 subsets of V γ 9V γ δ 2 effector cells with different responses and activation pathways. *Blood* **2004**, *104*, 1801–1807. [[CrossRef](#)] [[PubMed](#)]
43. Kohrt, H.E.; Houot, R.; Marabelle, A.; Cho, H.J.; Osman, K.; Goldstein, M.; Levy, R.; Brody, J. Combination strategies to enhance antitumour ADCC. *Immunotherapy* **2012**, *4*, 511–527. [[CrossRef](#)] [[PubMed](#)]
44. Carter, P.J.; Rajpal, A. Designing antibodies as therapeutics. *Cell* **2022**, *185*, 2789–2805. [[CrossRef](#)] [[PubMed](#)]
45. Vanneman, M.; Dranoff, G. Combining immunotherapy and targeted therapies in cancer treatment. *Nat. Rev. Cancer* **2012**, *12*, 237–251. [[CrossRef](#)] [[PubMed](#)]
46. Garvey, C.M.; Lau, R.; Sanchez, A.; Sun, R.X.; Fong, E.J.; Doche, M.E.; Chen, O.; Jusuf, A.; Lenz, H.J.; Larson, B.; et al. Anti-EGFR Therapy Induces EGF Secretion by Cancer-Associated Fibroblasts to Confer Colorectal Cancer Chemoresistance. *Cancers* **2020**, *12*, 1393. [[CrossRef](#)] [[PubMed](#)]

Disclaimer/Publisher's Note: The statements, opinions and data contained in all publications are solely those of the individual author(s) and contributor(s) and not of MDPI and/or the editor(s). MDPI and/or the editor(s) disclaim responsibility for any injury to people or property resulting from any ideas, methods, instructions or products referred to in the content.